

Article

Distributions, Relationship and Assessment of Major Ions and Potentially Toxic Elements in Waters of Bosten Lake, the Former Largest Inland and Freshwater Lake of China

Wen Liu ^{1,2,3} , Long Ma ^{1,2,3,*} , Jilili Abuduwaili ^{1,2,3}  and Lin Lin ⁴

¹ State Key Laboratory of Desert and Oasis Ecology, Xinjiang Institute of Ecology and Geography, Chinese Academy of Sciences, Urumqi 830011, China; liuwen@ms.xjb.ac.cn (W.L.); jilil@ms.xjb.ac.cn (J.A.)

² Research Center for Ecology and Environment of Central Asia, Chinese Academy of Sciences, Urumqi 830011, China

³ University of Chinese Academy of Sciences, Beijing 100049, China

⁴ Water Research Institute of Shandong Province, Jinan 250014, China; llin_mail@126.com

* Correspondence: malong@ms.xjb.ac.cn; Tel.: +86-991-7827371

Received: 31 August 2020; Accepted: 11 October 2020; Published: 14 October 2020



Abstract: As one of the important water sources of the desert ecosystem in the Tarim Basin, the largest fishery base in Xinjiang, and the former largest inland and freshwater lake of China, the water quality of Bosten Lake is worthy of government and public attention. To determine the water's hydrochemical composition and the water quality of Bosten Lake, analyses of the spatial distribution, water pollution status and irrigation suitability were conducted with statistical methods, including redundancy and factor analyses, inverse distance weighted interpolation, and water quality assessment and saturation index simulation of minerals in the water from a survey done in 2018. The results suggested that the average total dissolved solids (TDS) of Bosten Lake in 2018 was 1.32 g/L, and the lake is alkaline with a pH of 8.47. The strength of the water exchange capacity affected the spatial distribution of TDS. The spatial distribution of TDS and its value can be significantly changed by restoring the water supply of seasonal rivers in the northwest. The water of Bosten Lake contains sulfate and sodium groups, which are mainly affected by lake evaporation. As the pH increases, the content of carbonate ions increases, while the content of bicarbonate ions decreases. The spatial distributions of other major ions are consistent with that of the TDS. The spatial distribution of potentially toxic elements is more complicated than that of major ions. In general, the spatial distribution of Cu and As is more consistent with the spatial distribution of electrical conductivity or TDS. The spatial distributions of the Zn, Se and pH values are more consistent with respect to other variables. Although the water of Bosten Lake is still at a permissible level for water irrigation, the lake is moderately polluted, and the local site almost has a highly polluted status. The research results are of great significance for lake environmental protection and management as well as watershed ecological restoration.

Keywords: spatial distribution; potentially toxic elements; water quality; water pollution index; Bosten Lake; China

1. Introduction

With strong human activities superimposed on climate change, the lakes of Central Asia have experienced drastic changes, from lake surface expansion and water desalination to lake shrinkage and water salinization [1–3], especially for the Aral Sea [4]. Most of the lakes in the arid area are located at the tail of the river, which is the lowest catchment center in the region, receiving many kinds of

substances from the basin [5]. With the action of river inflow and dry and wet deposition, geochemical elements enter the lake [6]. Because a lake is a relatively closed natural water body with a long renewal cycle, the hydrodynamics inside the lake are not as extensive as those of flowing water bodies such as rivers, and potentially toxic elements (PTEs) in the water environment pose a high potential threat to the quality and safety of aquatic products because of their low degradability as well as their biotoxicity, bioaccumulation and biomagnification [7,8]. With the continuous increase in PTEs in lakes, lakes have become an important concentration area for PTEs in lake watersheds.

The research on Bosten Lake mainly focuses on the changes in the lake water level [9], as well as the physical, chemical and biological characteristics of water bodies, such as water and salt dynamics [10], weathering processes and water quality [11], and water microorganisms [12]. The regional paleoclimate and paleoenvironmental characteristics are reconstructed from the aspects of lake sediment grain size [13] and carbon isotopes [14]. Previous researchers conducted fruitful research on paleoenvironmental changes using lake sediment [15–22] and the modern ecology and environment of Bosten Lake [23–26], especially for surface sediments, e.g., studies of organic pollution [23,27], bacterial community [28–31], and PTE pollution [32–34]. Since the large-scale development of the Yanqi Basin, with the development of the economy and the enhancement of human activities, the discharge of industrial and agricultural wastewater and domestic water has intensified, and Bosten Lake has also been polluted [16]. Liu et al. [15] analysed the pollution level, source and change trend of heavy metals of Bosten Lake core sediments, and found that the pollution of PTEs has been aggravated over the past 50 years, which is mainly due to the use of phosphate fertilizer in regional agricultural activities. However, research on the water environment of lake water has not been carried out, which makes it impossible to understand the composition of major ions and the state of PTEs in the water of Bosten Lake.

Currently, it is urgent to study the major ions and PTEs in Bosten Lake waters. This is mainly based on the following two considerations. On the one hand, Bosten Lake is the largest natural water fishery base in Xinjiang [24]. The fluctuation of the lake water level causes drastic changes in the lake water quality, which seriously affects the output and quality of the lake fishery and directly affects the development of the local economy. In addition, as the largest fishery base in Xinjiang, the potentially toxic elements in the lake water also have a potential impact on human health. On the other hand, the main ion composition in the lake directly affects the irrigation suitability of the water body and then has an important impact on farmland and the downstream desert ecosystem restoration. Bosten Lake is the tail of the Kaidu River and one of the water sources of the Peacock River. With the decrease in the amount of water in Bosten Lake, the water of Bosten Lake can no longer naturally flow to the Peacock River. Since 1976, with the help of the pumping station and the main canal, Bosten Lake has been able to supply water to the Peacock River. The region of the Peacock River is a typical desert oasis and includes irrigated agricultural areas. The water sources in the irrigation area mainly come from river water and groundwater [35]. The water quality of Bosten Lake, which is an important part of the water source of the Peacock River, indirectly affects the safety of agricultural production. The desert riparian forest is dominated by *Populus euphratica* Oliv. in the middle and lower reaches of the Peacock River and the lower reaches of the Tarim River, forming a “green corridor” in the lower reaches of the Tarim River [36], which effectively prevented the closure of the two deserts of Taklimakan (in the west, the largest desert in China and world’s second-largest shifting sand desert [37,38]) and Kuluk (in the east, the third largest desert in China). From this, it can be seen that information on the water hydrochemical composition and the evaluation of the water quality of Bosten Lake have important application values for regional ecological and environmental protection.

To a large extent, the geochemical elemental composition of lake water bodies characterizes the environmental quality of lake water and reflects the environmental chemical characteristics of lake basins. Based on the above understanding and lake survey data of Bosten Lake, statistical methods and saturation index simulations of minerals are used to systematically analyse the characteristics of the main ion hydrochemistry and PTEs in the waters of Bosten Lake, to reveal the distribution law of

water elements, and to assess the water health status. The study will provide a scientific basis for lake environmental restoration and will improve the understanding of the environmental changes of lakes in central Asia.

2. Geographic Background

Bosten Lake is located at the south slope of the Tianshan Mountains. The elevation of Bosten Lake is about 1048 m [39]. The water area of the lake is approximately 1100 km², the volume is 88×10^8 m³, and the maximum water depth is 14 m [40]. It is currently the largest lake in the Xinjiang Uyghur Autonomous Region, China, and it was also the largest inland freshwater lake in China in the 1960s [29]; however, total dissolved solids (TDS) changed to 1.48 g/L in 2008 [16]. The catchment area of the basin is 5.5–105 km². The rivers that flow into Bosten Lake are the Kaidu River, and the Huangshui River, and only the Kaidu River is perennial [13]. The Kaidu River originates from the snowy mountains in the west; its water source is supplied by mountain precipitation and meltwater of ice and snow, and the total length of this river is 513 km [41], with an annual runoff of 3.99 billion cubic metres [42]. The water flows out of the lake into the Peacock River with the lifting hub of the west pumping station at the southwestern corner of Bosten Lake [16]. The lake is divided into a large lake region and a small lake district. The small lake district is located in the southwest and is a wetland rich in reeds. After 1983, the construction of the dam completely cut off the hydraulic connection between the southwest of the large lake region and the small lake district. In 2000, the Kaidu River entered the high water period: a large amount of fresh water entered Bosten Lake, the water level of the lake rose to 1048.45 metres, the TDS of the lake water decreased to 1.2 g/L, and in 2002, the lake water level reached the highest level of 1049.36 m [10]. In the same period, emergency water was transported to the lower reaches five times from May 2000 to November 2003, and a total of 2.22 billion m³ of water was transferred from the lake, which effectively alleviated the trend of serious deterioration of the ecological environment in the Tarim Basin, one of the largest inland basins in the world [43]. However, in recent years, especially since 2006, the river water entering Bosten Lake has significantly decreased, and the water level of the lake dropped to 1046.8 m in 2015, which is approximately 2 m lower than that in 2000 [29].

3. Materials and Methods

3.1. Sampling and Analytical Techniques

According to the shape of Bosten Lake, 33 sampling points were selected in September 2018; the locations of the sampling points are shown in Figure 1. A multipoint mixed sampling method was used (three parallel samples were collected from the same sampling point, and one sample was mixed in the field), and each sample area was approximately 5 × 5 m. The sampling bottle was a polyethylene plastic bottle. Before sampling, the sample bottle was soaked in 10% nitric acid for 24 h and rinsed with deionized water. During sampling, the bottle was rinsed with lake surface water 3 times. The samples of surface water (at a depth of 50 cm underwater) were collected. Among them, the samples for cations and PTEs were filtered through a 45 µm filter (Puradisc 25PP, Whatman International Ltd., Kent, UK) and immediately acidified with nitric acid to pH < 2. The pH of the surface water was measured using an S20 SevenEasy pH meter (Mettler-Toledo International Inc., Greifensee, Switzerland). Electrical conductivity (EC) and total dissolved solids (TDS_{obs}) were measured with a conductivity tester DDSJ-308A (Shanghai Precision & Scientific Instrument Co., Shanghai, China). The contents of PTEs (Cu, Ni, Cr, Pb, Cd, Zn, As, and Se) were measured with an ICP-OES spectrometer (Agilent 735, Agilent Technologies, Santa Clara, USA). The detection limits for Cu, Ni, Cr, Pb, Cd, Zn, As, and Se were 0.015, 0.010, 0.011, 0.003, 0.002, 0.014, 0.004, and 0.012 µg/L, respectively. HCO₃⁻ and CO₃²⁻ were determined with a G20 titrator (Mettler Toledo AG, Greifensee, Switzerland). The Ca²⁺, K⁺, Mg²⁺, Na⁺, Cl⁻ and SO₄²⁻ were measured with a Dionex ICS 5000 ionic chromatography system (Thermo Fisher Scientific Inc., Waltham, MA, USA). The results showed that the percent charge–balance error [44] ranged from

1.8% to 3.8%, which is less than 5%. The above analysis was completed in the Analysis and Test Center of Xinjiang Institute of Ecology and Geography, Chinese Academy of Sciences. The TDS value was calculated by Equation (1) [45], and the difference between the measured value (TDS_{obs}) and the calculated value (TDS_{cal}) of the instrument was also compared.

$$TDS_{cal} \text{ (mg/L)} = Ca^{2+} + K^+ + Mg^{2+} + Na^+ + Cl^- + SO_4^{2-} + CO_3^{2-} + 0.5 \times HCO_3^- \quad (1)$$

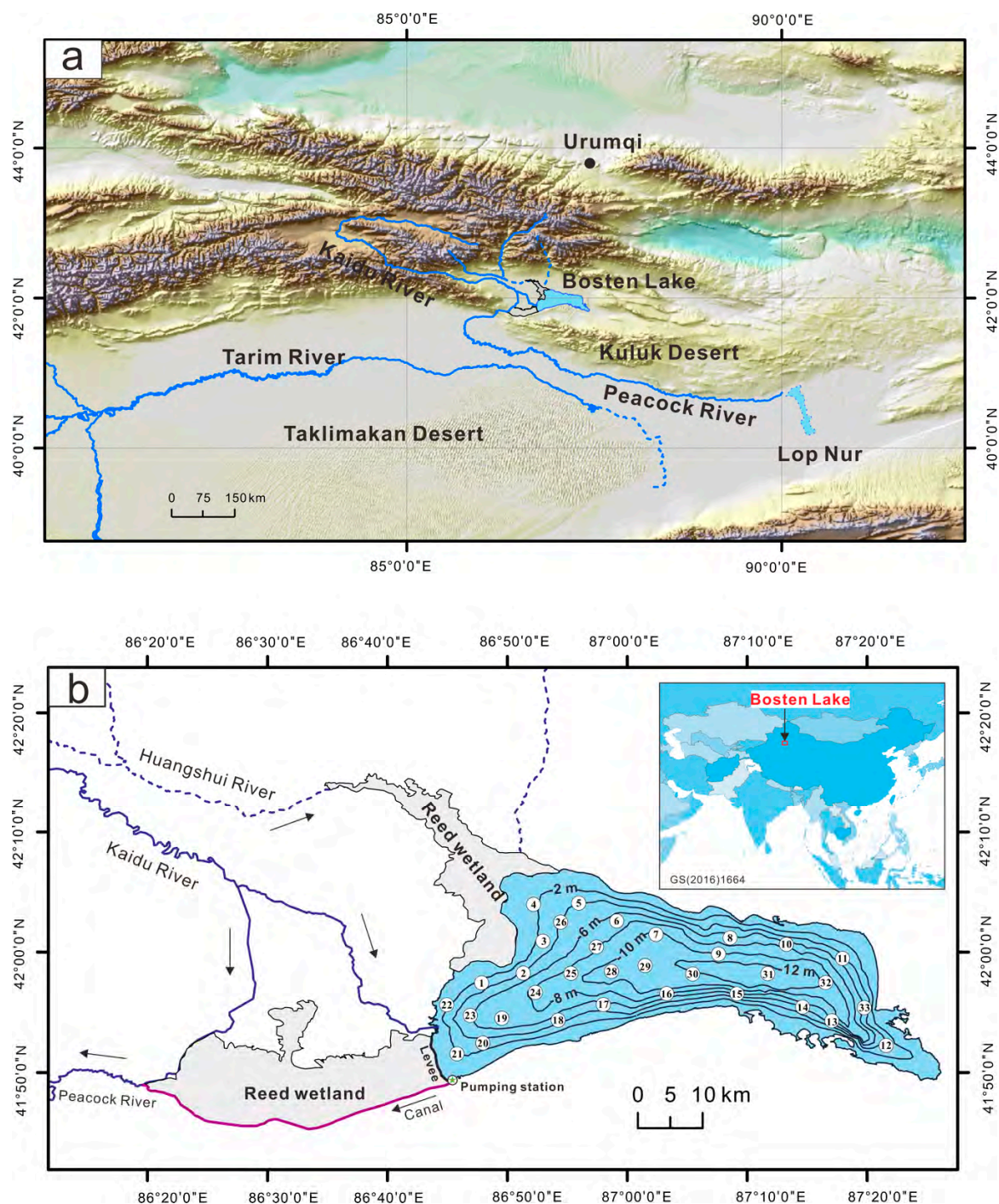


Figure 1. (a) The river water system of the Bosten Lake and (b) the distribution of sampling sites in Bosten Lake.

3.2. Assessment of Major Ions and Potentially Toxic Elements

The classification diagram from the United States Salinity Laboratory (USSL) [46,47] of EC vs. the sodium absorption ratio (SAR) [48,49] and the Wilcox diagram [50] of EC vs. the sodium percentage (Na %) [50–52] were used to evaluate the irrigation suitability of Bosten Lake water. For the whole chemical composition, the water pollution index (WPI) was used to assess the pollution status of Bosten Lake water. Hydrochemical parameters, including pH, EC, TDS, major ions (Na^+ , K^+ , Mg^{2+} , Ca^{2+} , HCO_3^- , CO_3^{2-} , Cl^- , and SO_4^{2-}), and PTEs (Cu, Ni, Cr, Pb, Cd, Zn, As, and Se), were used in the WPI method [53]. The calculation of WPI for one sampling point was as follows (Equations (2)–(4)):

$$\text{PLi} = \frac{C_i}{S_i} \quad (2)$$

$$\text{PLi} = \frac{C_i - 7}{S_{i_b} - 7} \quad (3)$$

$$\text{WPI} = \frac{1}{n} \sum_{i=1}^n \text{PLi} \quad (4)$$

where PLi is the pollution load for the *i*th parameter, C_i is the content of the *i*th parameter, and S_i is the highest permissible limit for the *i*th parameter from guidelines for drinking water quality from the World Health Organization (WHO) [54], and from the China National Standards for drinking-water quality (GB5749–2006) [55]. Examples of highest permissible parameter limits are: EC (750 $\mu\text{S}/\text{cm}$), TDS (500 mg/L), Na^+ (200 mg/L), K^+ (200 mg/L), Mg^{2+} (50 mg/L), Ca^{2+} (75 mg/L), HCO_3^- (240 mg/L), Cl^- (250 mg/L), SO_4^{2-} (250 mg/L), Cu (1000 $\mu\text{g}/\text{L}$), Ni (20 $\mu\text{g}/\text{L}$), Cr (50 $\mu\text{g}/\text{L}$), Pb (10 $\mu\text{g}/\text{L}$), Cd (5 $\mu\text{g}/\text{L}$), Zn (1000 $\mu\text{g}/\text{L}$), As (10 $\mu\text{g}/\text{L}$), and Se (10 $\mu\text{g}/\text{L}$). In this study, the pH in the waters of Bosten Lake was higher than 7, and the S_{i_b} in Equation (2) equalled 8.5 [53]. According to the WPI results, the water can be classified into four levels: excellent water (<0.5), good water (0.5–0.75), moderately polluted water (0.75–1), and highly polluted water (>1) [53].

3.3. Statistical Analyses

Factor analysis [56] for the data of pH, EC and major ions in Bosten Lake water, with the maximum variance method for rotation, and the the Kaiser–Meyer–Olkin (KMO) and Bartlett’s test result, were used to reveal the influencing factors for pH and EC in Bosten Lake water. Redundancy analysis (RDA) was used to reveal possible factors for the PTEs, and the RDA was done by Canoco 5 [57], with no data transformation and unrestricted permutations (number of permutations was 499). The spatial distribution for pH, EC, TDS, major ions and PTEs was used with the inverse distance weighted interpolation method [58].

4. Results

Because the observed values (TDS_{obs}) were converted from the associated parameters of the measuring instrument, they cannot truly reflect the real situation of Bosten Lake, as there is a large difference between the observed value (TDS_{obs}) and the calculated value (TDS_{cal}) (Table 1, Figure 2). The TDS_{cal} of Bosten Lake can reflect the real value, which varied from 1.07 to 1.47 g/L, with an average of 1.32 g/L (Table 1), and the calculated value shows that the water of Bosten Lake is brackish. The pH of Bosten Lake varies from 8.35 to 8.54, with an average of 8.47 (Table 1), suggesting that Bosten Lake is alkaline. The EC of Bosten Lake varies from 1282 to 1636 $\mu\text{S}/\text{cm}$ (Table 1).

The cation Na^+ in the waters of Bosten Lake is the main cation (Table 1 and Figure 3), with a concentration ranging from 8.52 to 11.80 meq/L (Table 1), accounting for 22.65% of the total ions (Figure 3). SO_4^{2-} is the main anion, ranging from 7.41 to 10.84 meq/L, accounting for 19.80% of the total ions (Figure 3). The order of ion concentration is CO_3^{2-} (mean value, 0.62 meq/L), K^+ (2.59 meq/L),

Ca²⁺ (3.57 meq/L), HCO₃⁻ (4.67 meq/L), Cl⁻ (7.70 meq/L), Mg²⁺ (8.32 meq/L), SO₄²⁻ (9.46 meq/L), and Na⁺ (10.81 meq/L).

Table 1. Descriptive statistics and normality test (Kolmogorov–Smirnov) of the hydrochemical parameters of Bosten Lake (n = 33).

Parameter	Unit	Minimum	Maximum	Mean	Standard Error	Standard Deviation	Kolmogorov–Smirnov Test	p
pH		8.35	8.54	8.4652	0.008	0.044	0.11	0.86 ^b
EC	μS/cm	1282	1636	1529.85	11.942	68.603	0.32	0 ^a
TDS _{obs}	mg/L	1312	1672	1562.73	12.484	71.713	0.31	0 ^a
TDS _{cal}	mg/L	1067.7	1474.46	1324.34	13.03	74.83	0.28	0.01 ^a
Cl ⁻	mg/L	210.61	321.03	272.87	3.46	19.87	0.25	0.02 ^a
SO ₄ ²⁻	mg/L	355.69	520.51	454.19	5.32	30.54	0.24	0.03 ^a
Ca ²⁺	mg/L	65.76	73.32	71.58	0.27	1.54	0.25	0.03 ^a
K ⁺	mg/L	11.85	17.43	15.04	0.17	0.97	0.28	0.01 ^a
Mg ²⁺	mg/L	80.93	110.08	101.1	0.99	5.7	0.31	0.00 ^a
Na ⁺	mg/L	195.85	271.31	248.5	2.39	13.73	0.3	0.00 ^a
CO ₃ ²⁻	mg/L	9.33	25.75	18.65	0.73	4.19	0.07	1.00 ^b
HCO ₃ ⁻	mg/L	270.59	310.21	284.81	1.42	8.17	0.09	1.00 ^b
Cu	μg/L	2.932	3.685	3.428	0.021	0.123	0.19	0.16 ^b
Ni	μg/L	3.308	4.269	3.923	0.037	0.215	0.13	0.63 ^b
Cr	μg/L	1.351	3.824	2.515	0.124	0.71	0.08	1.00 ^b
Pb	μg/L	0.072	0.265	0.131	0.008	0.046	0.17	0.25 ^b
Cd	μg/L	0.007	0.028	0.016	0.001	0.005	0.1	0.99 ^b
Zn	μg/L	1.291	10.546	4.213	0.44	2.529	0.21	0.09 ^b
As	μg/L	10.217	13.87	11.669	0.141	0.808	0.11	0.78 ^b
Se	μg/L	0.787	1.273	0.938	0.018	0.106	0.15	0.41 ^b
Cl ⁻	meq/L	5.94	9.06	7.7	0.1	0.56	/	/
SO ₄ ²⁻	meq/L	7.41	10.84	9.46	0.11	0.64	/	/
Ca ²⁺	meq/L	3.28	3.66	3.57	0.01	0.08	/	/
K ⁺	meq/L	2.07	2.82	2.59	0.03	0.15	/	/
Mg ²⁺	meq/L	6.66	9.06	8.32	0.08	0.47	/	/
Na ⁺	meq/L	8.52	11.8	10.81	0.1	0.6	/	/
CO ₃ ²⁻	meq/L	0.31	0.86	0.62	0.02	0.14	/	/
HCO ₃ ⁻	meq/L	4.44	5.08	4.67	0.02	0.13	/	/

^a Reject normality; ^b Cannot reject normality.

Lake water chemistry types are usually classified according to the main anions and cations and the relationship between the ions. Water samples can be divided into three types according to the main anions: bicarbonate and carbonate (CO₃²⁻ + HCO₃⁻) type, sulfate (SO₄²⁻) type and chloride (Cl⁻) type. The main cations are divided into 3 groups: calcium (Ca²⁺), magnesium (Mg²⁺) and sodium (Na⁺). According to the classification of the Piper diagram [59], the water of Bosten Lake contains sulfate and sodium (Figure 4). Each group is divided into 4 types according to the contrast relationship between ions: Type I: HCO₃⁻ > Ca²⁺ + Mg²⁺, mostly low-mineralized water; Type II: HCO₃⁻ < Ca²⁺ + Mg²⁺ < HCO₃⁻ + SO₄²⁻, mostly medium-, low-mineralized water; Type III: HCO₃⁻ + SO₄²⁻ > Ca²⁺ + Mg²⁺ or Cl⁻ > Na⁺, high TDS; Type IV: HCO₃⁻ = 0 indicates acidic water. The Bosten Lake water was classified as follows: HCO₃⁻ < Ca²⁺ + Mg²⁺ < HCO₃⁻ + SO₄²⁻, which means that Bosten Lake water belongs to the sulfate, sodium group belonging to Type II (HCO₃⁻ < Ca²⁺ + Mg²⁺ < HCO₃⁻ + SO₄²⁻), reflecting a medium, low-mineralized status.

The average contents of Cu, Ni, Cr, Zn and Se are of the same order of magnitude (Figure 5). Among the potentially toxic elements in Bosten Lake, arsenic has the highest content, with an average content of 11.669 μg/L. The lowest contents were found for lead and cadmium, with average contents of 0.265 and 0.028 μg/L, respectively (Table 1).

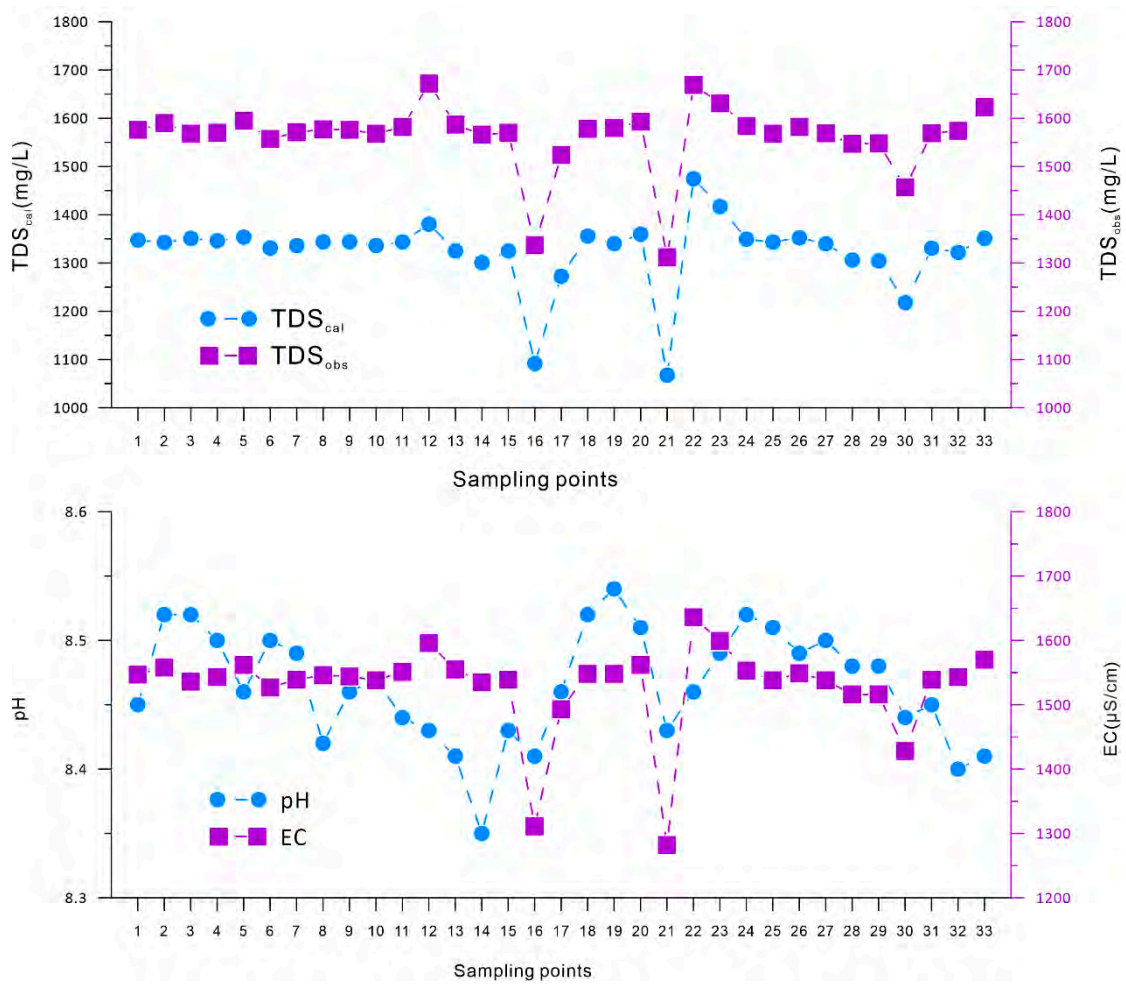


Figure 2. The values of pH, electrical conductivity (EC), observed values of total dissolved solids (TDS_{obs}) and calculated values of total dissolved solids (TDS_{cal}) for Bosten Lake waters at different sampling points.

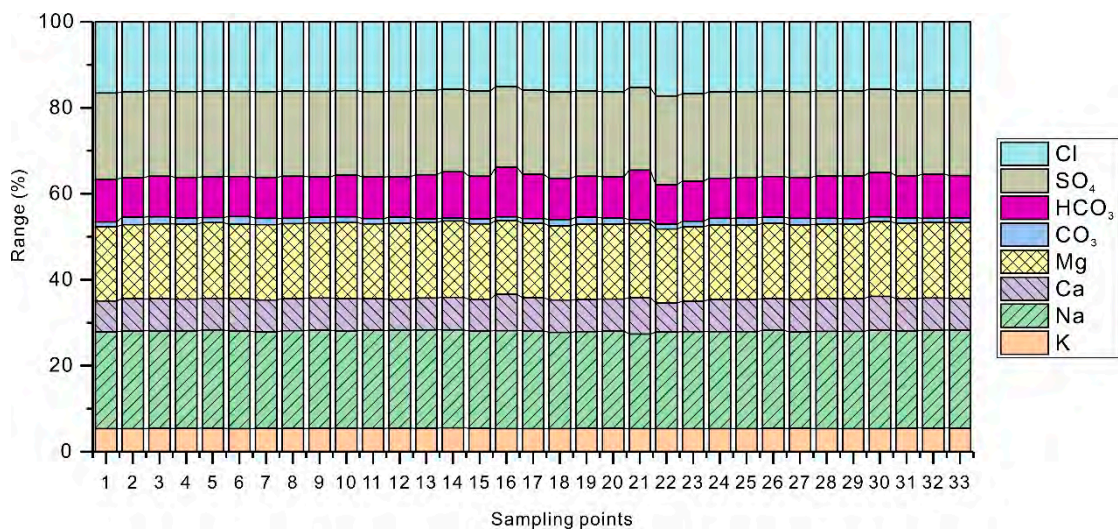


Figure 3. The percentage of equivalent weight of major ions in Bosten Lake waters at different sampling points.

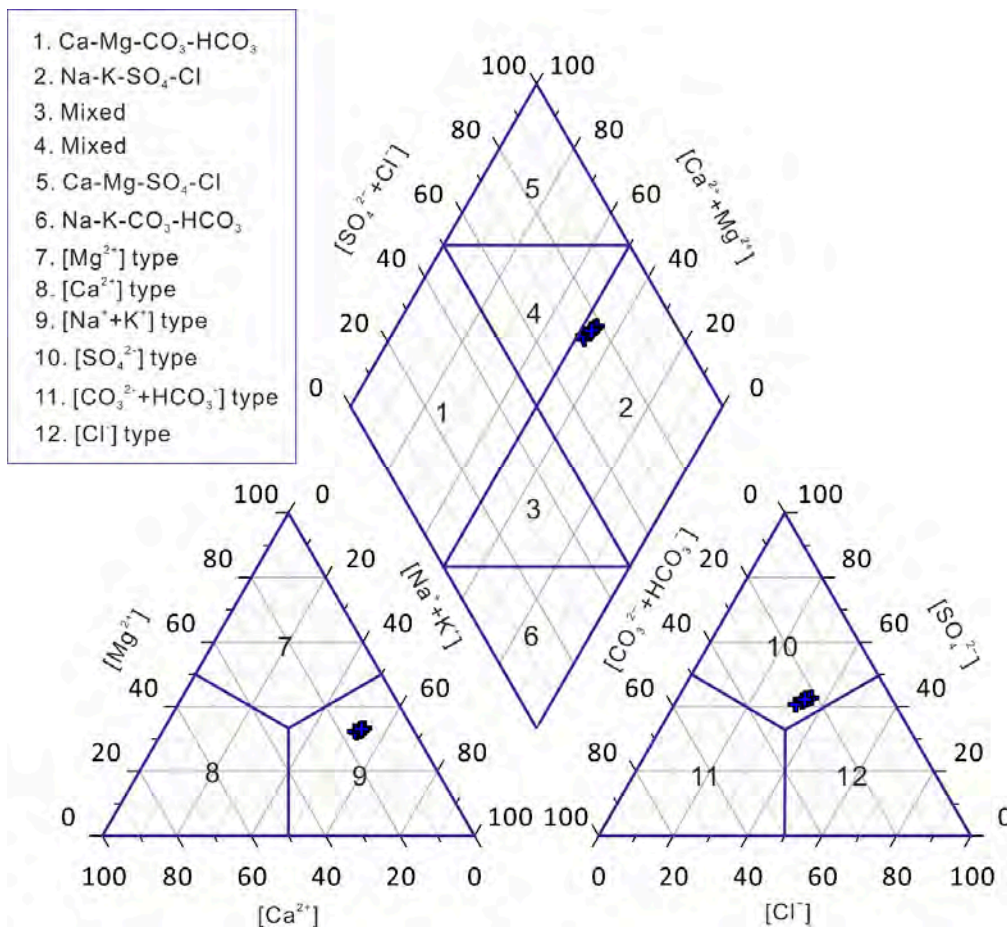


Figure 4. Piper diagram of the waters from Bosten Lake.

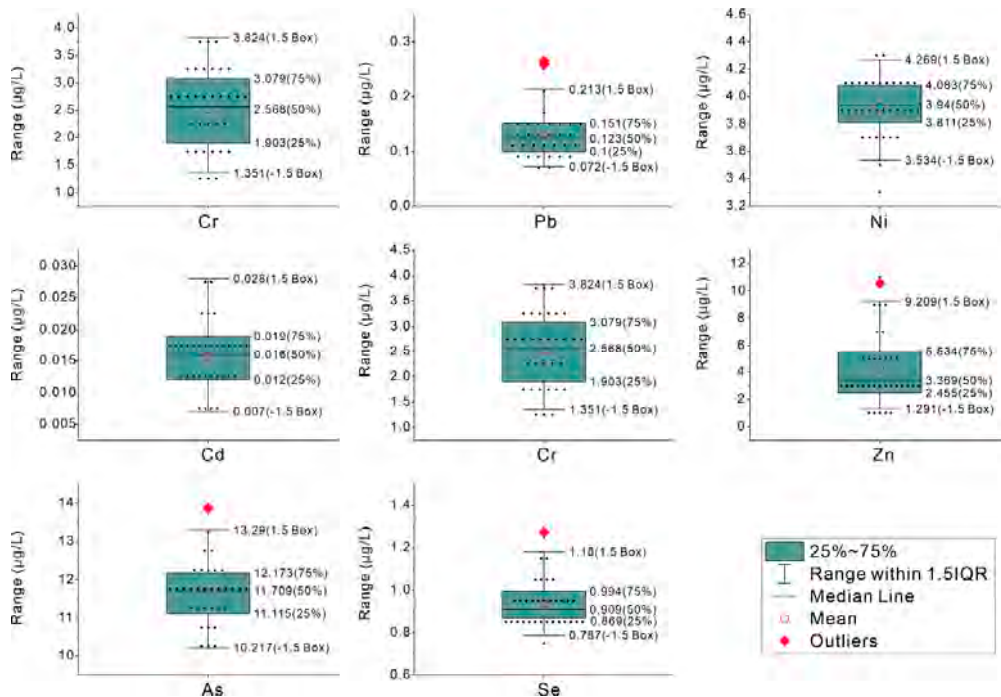


Figure 5. Vertical box plots showing the range of potentially toxic elements (PTEs) in the waters of Bosten Lake (n = 33).

5. Discussion

With respect to factor analysis of pH, EC and major ions in Bosten Lake water with the maximum variance method for rotation, the Kaiser–Meyer–Olkin (KMO) and Bartlett’s test result with value of 0.869 meet the factor analysis conditions. Therefore, according to the results of factor analysis [56], 2 categories were obtained (Figure 6), corresponding to F1 and F2, which together explain 92.75% of the total variance. The loading coefficients of Ca^{2+} , K^+ , Mg^{2+} , Na^+ , Cl^- , and SO_4^{2-} are high on the F1 factor, i.e., all above 0.9, which explains 67.82% of the change. This reflects that the EC in Bosten Lake water is mainly affected by the content of these ions. The F2 factor has a high CO_3^{2-} loading coefficient of 0.74, which explains 24.93% of the variation. HCO_3^- and CO_3^{2-} show a negative correlation, and the loading coefficient of HCO_3^- on F2 is -0.934 . When $10 > \text{pH} > 8.3$, HCO_3^- and CO_3^{2-} exist simultaneously [60]. The pH value is one of the main indicators of the overall condition and material composition of the water environment, and it controls the migration and transformation of various substances in the water body. The pH of Bosten Lake is between 8.35 and 8.54. As the pH increases, the content of carbonate ions increases, while the content of bicarbonate ions decreases.

From the perspective of the spatial distribution with the inverse distance weighted interpolation method [58] for pH, EC, TDS and major ions (Figure 7), the pH distribution of Bosten Lake varies significantly from east to west. The pH value in the east of the lake area was higher than that in the west (Figure 7). The highest TDS appears in the west of the lake (the highest was sampling point 22 in Figure 1), and the lowest value of TDS appears in the center of the lake and southwest (sampling point 21) (Figure 7). The exchange capacity of the water in the middle and east of the lake area is weak, so the lake water TDS is unevenly distributed. It is very interesting that the highest point and lowest point of the conductivity of Bosten Lake water are located at the parts between the inlet and the outlet, located in a small area in the southwest of the great lake. This results in the strongest water cycle in the southwestern part and the lowest EC and TDS in this part. However, in the western and eastern regions, due to the internal circulation of the lake, the injection of fresh water is relatively small, resulting in an increase in the EC and TDS of the lake water.

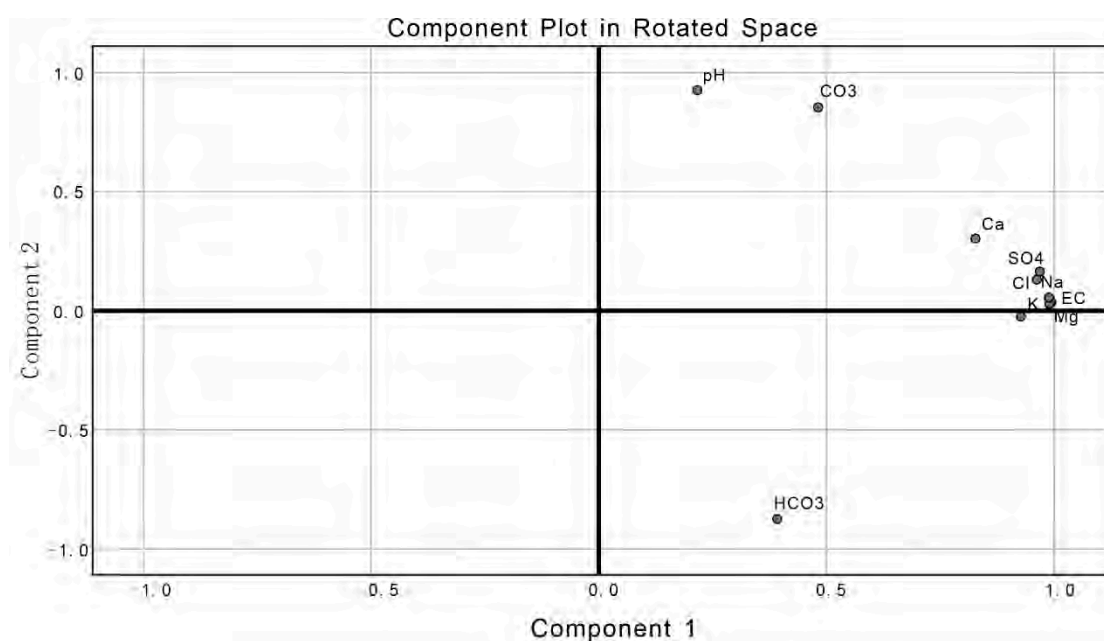


Figure 6. Loading coefficients for pH, EC and major ions in Bosten Lake water, based on factor analysis.

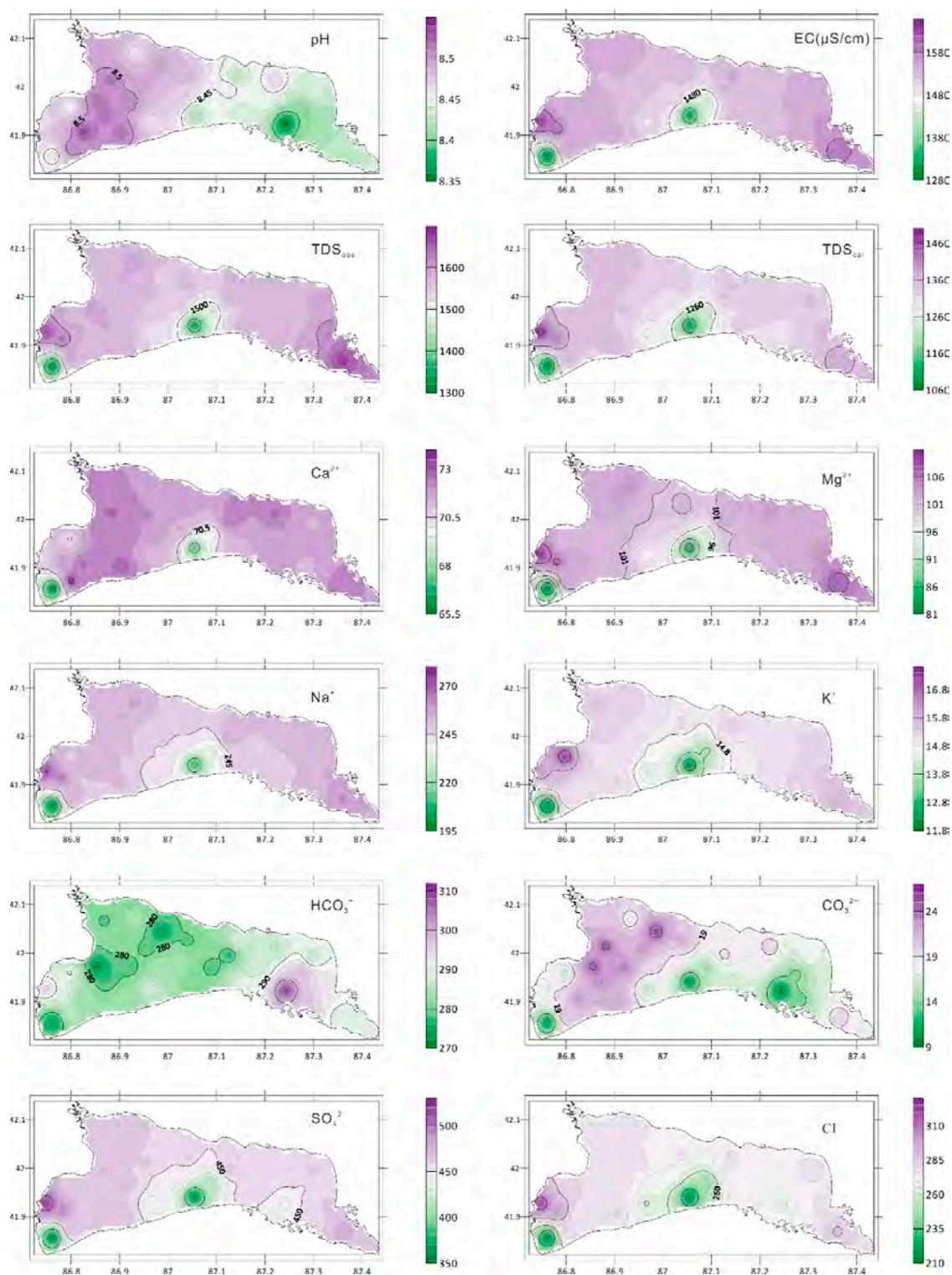


Figure 7. The distribution maps of pH, electrical conductivity (EC), measured value of total dissolved solids (TDS_{obs}), the calculated value (TDS_{cal}), and major ions in Bosten Lake water.

Gibbs diagrams [61–63] reflect three natural processes for water. It can be seen from Figure 8 that the composition of the main ions of Kaidu River water, the source of Bosten Lake, is dominated by rock. After the river flows into the lake, the water of Bosten Lake is significantly affected by evaporation. Under the effect of evaporation and concentration, some minerals in the lake water body reach a supersaturated state, and chemical precipitation occurs. Through the calculation of the saturation

indices by the PHREEQC program [64], it was found that the carbonate minerals (aragonite, calcite and dolomite) are in a supersaturated state (Figure 9), and endogenous carbonate precipitation occurs in Bosten Lake.

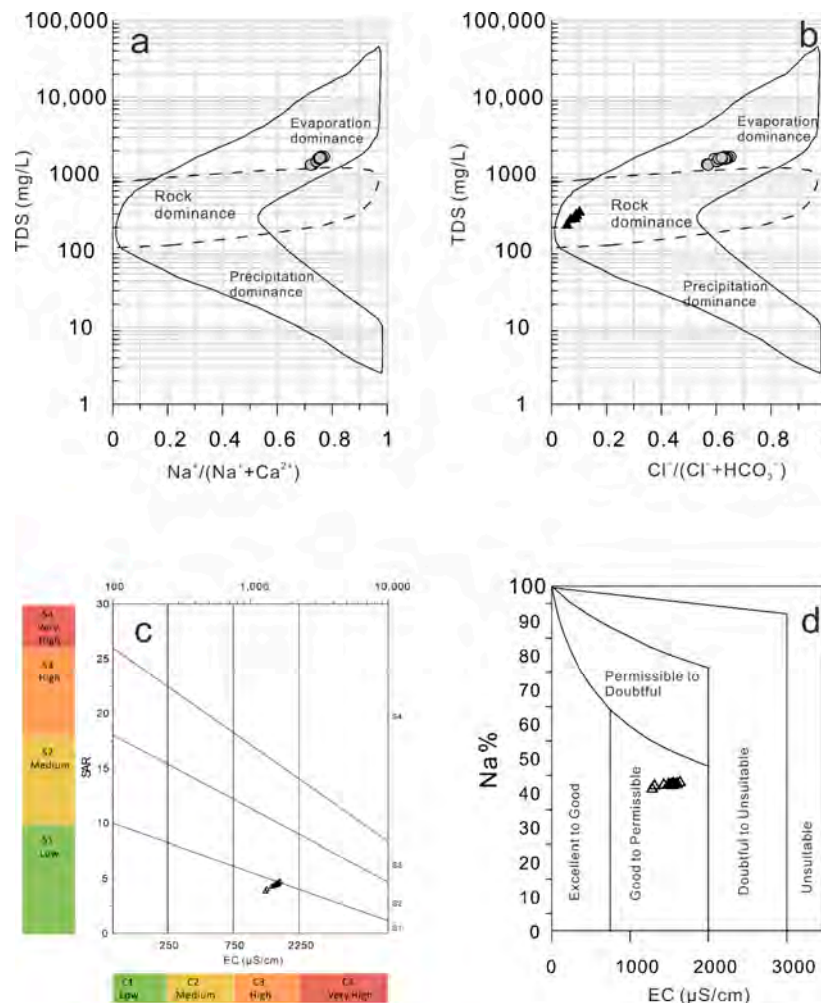


Figure 8. Gibbs diagrams (a,b) for river water and lake water in the Bosten Lake basin (circles represent Bosten Lake water, and triangles represent Kaidu River water [65]) and the assessment of the irrigation suitability of Bosten Lake water; (c) classification diagram from the United States Salinity Laboratory with EC vs. the sodium absorption ratio (SAR) and (d) Wilcox diagram with EC vs. the sodium percentage (Na%).

The Peacock River is mainly composed of the Kaidu River and Bosten Lake. Although the water of Bosten Lake is not directly used for irrigation, the Bosten Lake water flows into the Peacock River through the pumping station, which is of great significance for the irrigation of downstream farmland and the restoration of desert vegetation. The SAR and Na % indicated the sodium hazard. A high content of Na^+ will deteriorate the soil texture, making it difficult to permeate water and air and thereby will severely reduce soil water availability, which is detrimental to crop growth [66]. From the classification diagrams (Figure 8), the Bosten Lake water belongs to categories C3-S1, but one sample is located in the area C3-S2. The Wilcox diagram suggests that the irrigation water quality is good to permissible, and infers that the water is suitable for irrigation.

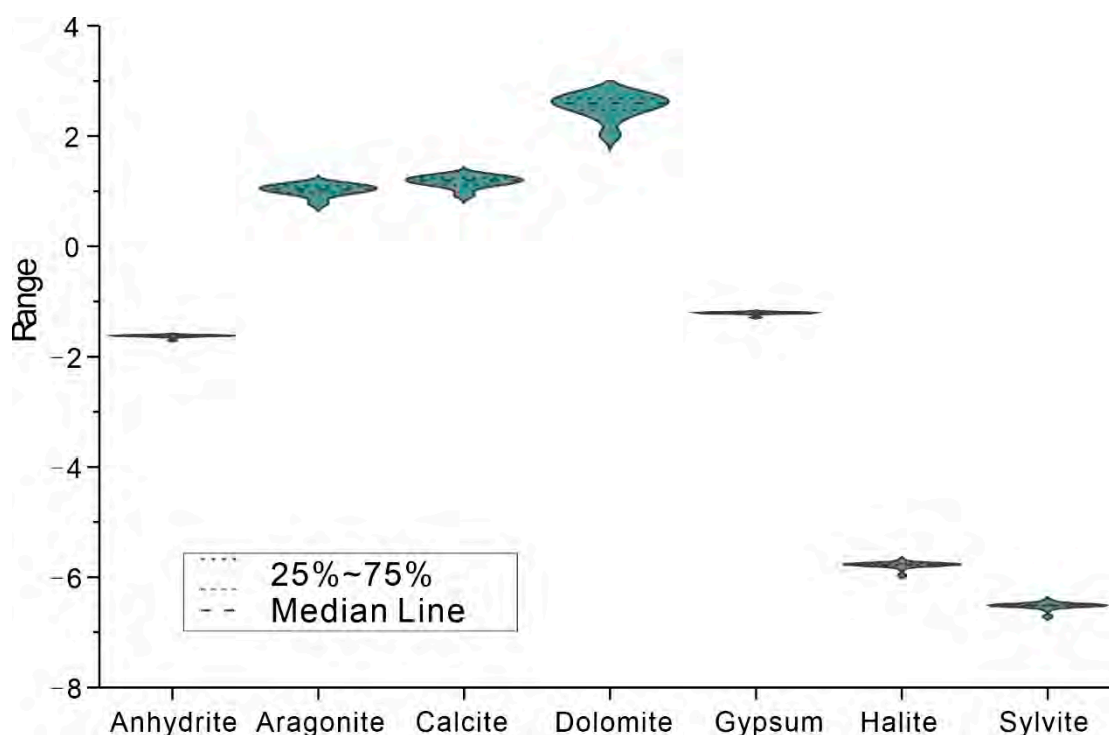


Figure 9. The results of the saturation index simulation of minerals in Bosten Lake.

Based on the spatial distribution of PTEs in the Bosten Lake waters (Figure 10), the content of Ni in the north-western part of the lake is relatively low. The content of Cd is higher in the eastern and western parts and lower in most areas in the middle of the lake. Spatially, low-value areas of Cu appear in the central and western regions. The high-value area appears in the west, which is similar to the spatial distribution map of electrical conductivity. The spatial distribution of As is basically the same as that of Cu, and low-value areas also appear in the central and western regions. Although Cr has low-value areas in the central and southern regions, its low-value areas are widely distributed. It can also be seen from the redundancy analysis graph that Cu and As are closely related to EC. The distribution of Pb is in the opposite direction of that of Cu and As, and high-value areas appear in the central and southern regions. The spatial distributions of Zn and Se are very similar. On the whole, the Zn and Se in the east of the lake are low, while in the west, the contents are high. Through redundancy analysis [67–72] with the software Canoco 5.0 [57], the changes in Zn and Se are closely related to pH (Figure 11). However, whether this reflects that the pH value of lake water affects the content of Zn and Se is still uncertain because changes in the contents of CO_3^{2-} and HCO_3^- in the lake lead to changes in the pH value. Zn and Se easily combine with CO_3^{2-} ions in lake water, causing the lake pH to change consistently with Zn and Se.

Although the assessment of the irrigation suitability of Bosten Lake water indicated suitability for irrigation, the analysis of the water pollution index shows that Bosten Lake is moderately polluted (Figure 12), and the WPI value ranges from 0.72 to 0.95. Individual locations have WPI values close to 1 (highly polluted). Among the 33 sampling points, only two points have a WPI value less than 0.75, which is a good level. The toxic effects of PTEs on aquatic plants are mainly manifested in changing the microstructure of cells, inhibiting photosynthesis, respiration, and enzyme activity, changing the composition of nucleic acids, and reducing cell volume and inhibiting growth [73]. After PTEs enter the water body, they will have a series of effects on the growth and development and physiological metabolism of aquatic animals [74]. Due to the concentration of the food chain, once humans eat these foods, PTEs will interact strongly with proteins and various enzymes in the human body, making proteins and enzymes inactive, and may also be enriched in certain organs of the human body, which will cause acute, subacute and chronic poisoning [74]. As the PTE levels exceed the World Health

Organization (WHO) guideline level [54], even the minimum level is above 10 ug/L. Existing studies on As in surface water and groundwater in Central Asia show that the same phenomenon was reported for the Aral Sea and one of its inflowing rivers [75], and the arsenic pollution in groundwater of Central Asia has a high probability of causing harm [76]. Limited to the data currently available, it is impossible to trace the source of As. This phenomenon of high concentration for As in central Asia requires great attention, which requires more in-depth research on its form and source in the future. Due to the increase in water consumption in the basin caused by human activities, the amount of water entering the lake has been significantly reduced, the area of the lake has shrunk, and the salt content of the lake has increased since the 1960s. Bosten Lake changed from the largest freshwater lake in inland China in the 1960s to a brackish lake. Its impact on the lake aquatic ecosystem and the downstream desert ecosystem is bound to be far-reaching. From the perspective of the spatial distribution of the water pollution index, the water bodies are cleaner in the southwestern region where the exchange of water bodies is strong. The eastern and western regions with poor water exchange capacity are more polluted. Humans should increase the water replacement capacity of the lake through the water supply of the Huangshui River (Figure 1) during social development, and reduce lake pollutants.

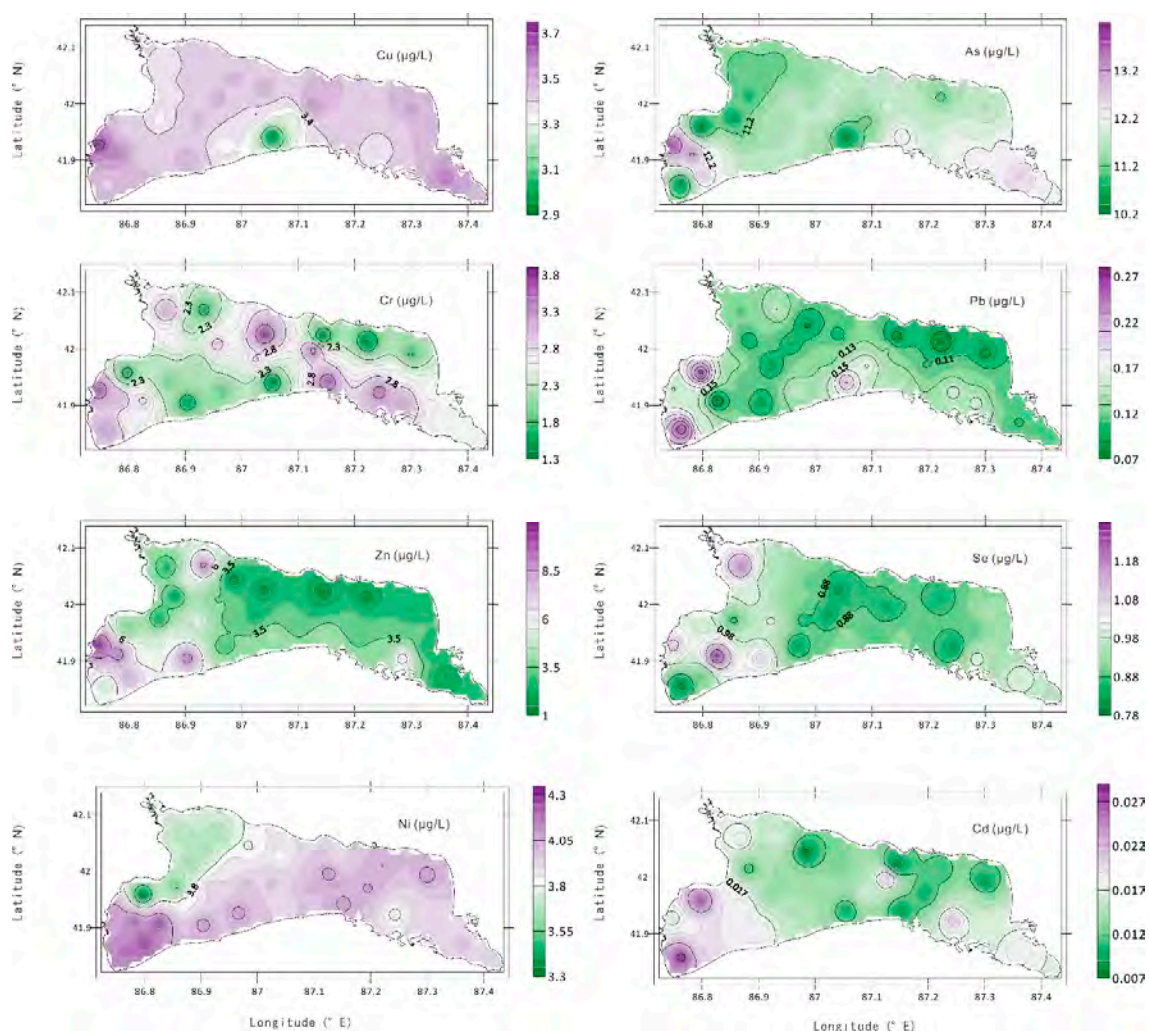


Figure 10. Spatial distribution maps of PTEs in Bosten Lake water.

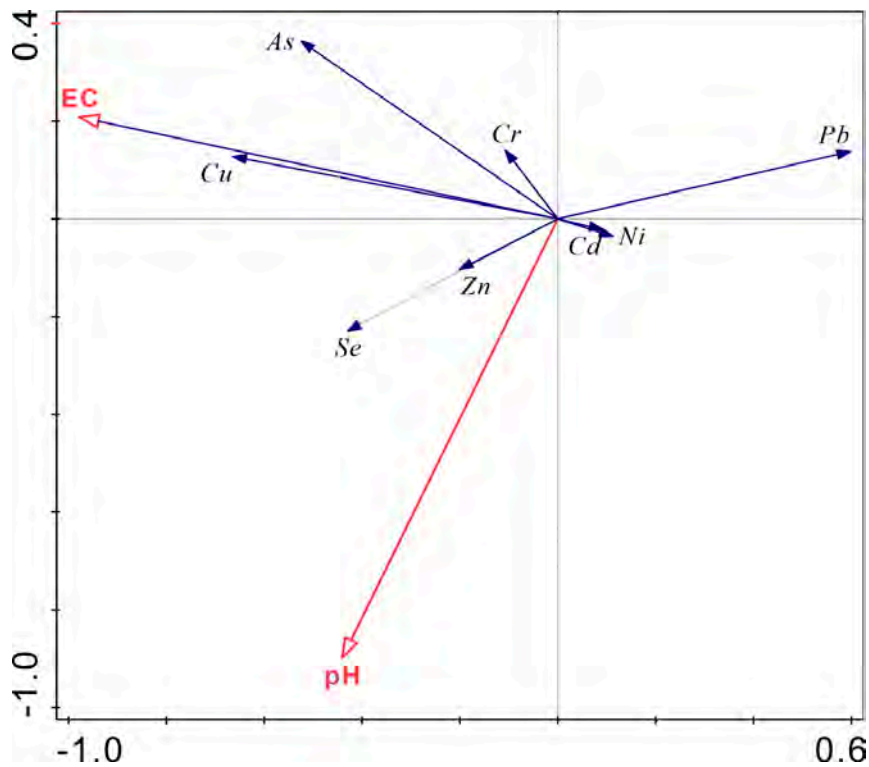


Figure 11. Redundancy analyses for the correlation between the pH, EC and the potential toxic elements in the waters of Bosten Lake.

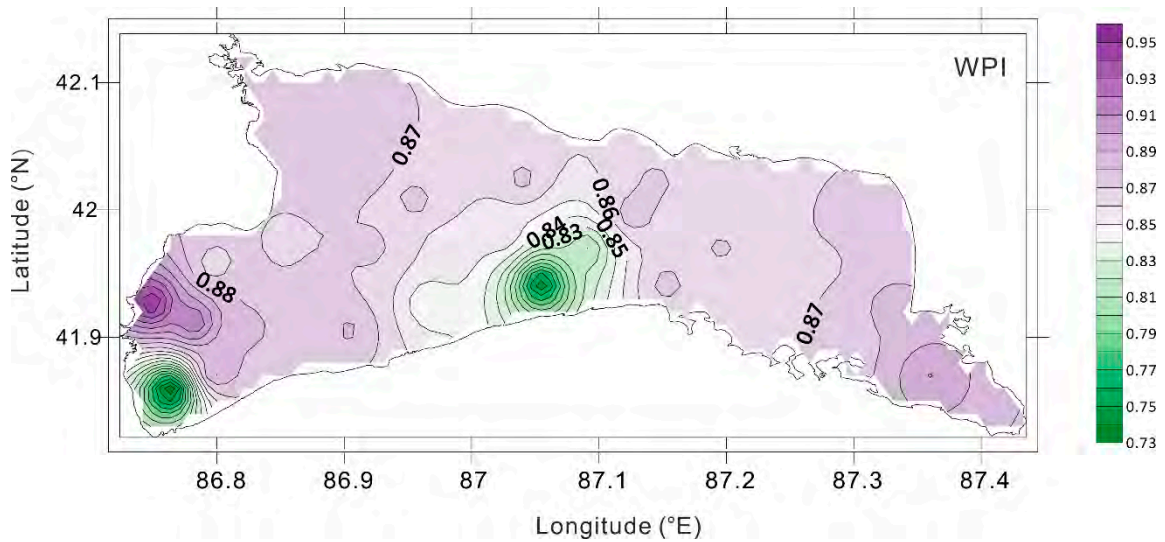


Figure 12. Spatial distribution maps of the water pollution index (WPI), in Bosten Lake.

6. Conclusions

- (1) The average TDS of Bosten Lake in 2018 was 1.56 g/L and 1.32 g/L for the measured and calculated values, respectively. The average pH value of the lake water body is 8.47, indicating this is an alkaline lake. The water type of Bosten Lake belongs to the sulfate, sodium group, type II ($\text{HCO}_3^- < \text{Ca}^{2+} + \text{Mg}^{2+} < \text{HCO}_3^- + \text{SO}_4^{2-}$).
- (2) From the perspective of spatial distribution, as the pH increases, the content of carbonate ions increases, while the content of bicarbonate ions decreases. The composition of other major ions is consistent with the change in the TDS. The spatial distribution of potentially toxic elements is

more complicated. In general, the spatial distribution of Cu and As is more consistent with EC or TDS. The spatial distributions of Zn, Se and pH values are more consistent. The strength of the water exchange capacity may affect the spatial distribution of the TDS. The lake water chemistry is mainly affected by lake evaporation.

- (3) Based on a combination of the EC, SAR and Na %, the water of Bosten Lake is still at a permissible level for water irrigation; however, the evaluation of water pollution combined with pH, TDs, EC, major ions, and potentially toxic elements shows that Bosten Lake is moderately polluted and that the local site is close to a high pollution status. As one of the important water sources in the desert ecosystem of the Tarim Basin and the largest fishery base in Xinjiang, China, this pollution status is worthy of government and public attention.

Author Contributions: Conceptualization, L.M. and J.A.; methodology, L.M. and L.L.; validation, L.M. and J.A.; investigation, L.M. and W.L.; data curation, W.L.; writing—original draft preparation, L.M. and W.L.; writing—review and editing, L.M. and J.A.; visualization, W.L.; supervision, L.M.; project administration, L.M. and J.A.; funding acquisition, L.M., L.L. and J.A. All authors have read and agreed to the published version of the manuscript.

Funding: This research is funded by the National Natural Science Foundation of China (U1903115), the Chinese Academy of Sciences (2019000058), the Tianshan Youth Project of Xinjiang Uygur Autonomous Region of China (2018Q008), the High-level Training Project of Xinjiang Institute of Ecology and Geography, CAS (E050030101), and the Shandong provincial water resources research project (SDSLKY201813).

Conflicts of Interest: The authors declare no conflict of interest.

References

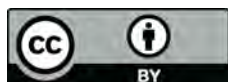
1. Wurtsbaugh, W.A.; Miller, C.; Null, S.E.; DeRose, R.J.; Wilcock, P.; Hahnenberger, M.; Howe, F.; Moore, J. Decline of the world's saline lakes. *Nat. Geosci.* **2017**, *10*, 816–821. [[CrossRef](#)]
2. Pekel, J.-F.; Cottam, A.; Gorelick, N.; Belward, A.S. High-resolution mapping of global surface water and its long-term changes. *Nature* **2016**, *540*, 418–422. [[CrossRef](#)]
3. Wang, J.; Song, C.; Reager, J.T.; Yao, F.; Famiglietti, J.S.; Sheng, Y.; MacDonald, G.M.; Brun, F.; Schmied, H.M.; Marston, R.A.; et al. Recent global decline in endorheic basin water storages. *Nat. Geosci.* **2018**, *11*, 926–932. [[CrossRef](#)]
4. Aladin, N.V.; Gontar, V.I.; Zhakova, L.V.; Plotnikov, I.S.; Smurov, A.O.; Rzymiski, P.; Klimaszuk, P. The zoocenosis of the Aral Sea: Six decades of fast-paced change. *Environ. Sci. Pollut. Res.* **2019**, *26*, 2228–2237. [[CrossRef](#)]
5. Liu, H.; Chen, Y.; Ye, Z.; Li, Y.; Zhang, Q. Recent Lake Area Changes in Central Asia. *Sci. Rep.* **2019**, *9*, 16277. [[CrossRef](#)]
6. Jin, Z.; You, C.-F.; Yu, J. Toward a geochemical mass balance of major elements in Lake Qinghai, NE Tibetan Plateau: A significant role of atmospheric deposition. *Appl. Geochem.* **2009**, *24*, 1901–1907. [[CrossRef](#)]
7. Shakeri, A.; Fard, M.S.; Mehrabi, B.; Mehr, M.R. Occurrence, origin and health risk of arsenic and potentially toxic elements (PTEs) in sediments and fish tissues from the geothermal area of the Khiav River, Ardebil Province (NW Iran). *J. Geochem. Explor.* **2020**, *208*, 106347. [[CrossRef](#)]
8. Grygar, T.M.; Bábek, O.; Sedláček, J.; Lendáková, Z.; Faměra, M.; Štojdl, J.; Pacina, J.; Tolaszová, J.; Kříženecká, S. Segregation and retention of As, potentially toxic metals, and organic pollutants in a reservoir from the Ohře River (the Czech Republic). *J. Soils Sediments* **2020**, *20*, 2931–2948. [[CrossRef](#)]
9. Yao, J.; Chen, Y.; Zhao, Y.; Yu, X. Hydroclimatic changes of Lake Bosten in Northwest China during the last decades. *Sci. Rep.* **2018**, *8*, 9118. [[CrossRef](#)]
10. Rusuli, Y.; Li, L.; Ahmad, S.; Zhao, X. Dynamics model to simulate water and salt balance of Bosten Lake in Xinjiang, China. *Environ. Earth Sci.* **2015**, *74*, 2499–2510. [[CrossRef](#)]
11. Xiao, J.; Jin, Z.; Wang, J.; Zhang, F. Major ion chemistry, weathering process and water quality of natural waters in the Bosten Lake catchment in an extreme arid region, NW China. *Environ. Earth Sci.* **2015**, *73*, 3697–3708. [[CrossRef](#)]
12. Zhou, T.; Lu, J.; Tong, Y.; Li, S.; Wang, X. Distribution of antibiotic resistance genes in Bosten Lake, Xinjiang, China. *Water Sci. Technol.* **2014**, *70*, 925–931. [[CrossRef](#)] [[PubMed](#)]

13. Ma, L.; Abuduwaili, J.; Liu, W. Environmentally sensitive grain-size component records and its response to climatic and anthropogenic influences in Bosten Lake region, China. *Sci. Rep.* **2020**, *10*, 942. [[CrossRef](#)]
14. Zhang, C.; Mischke, S.; Zheng, M.; Prokopenko, A.; Guo, F.; Feng, Z. Carbon and Oxygen Isotopic Composition of Surface-Sediment Carbonate in Bosten Lake (Xinjiang, China) and its Controlling Factors. *Acta Geol. Sin.-Engl. Ed.* **2009**, *83*, 386–395. [[CrossRef](#)]
15. Liu, W.; Abuduwaili, J.; Ma, L. Geochemistry of major and trace elements and their environmental significances in core sediments from Bosten Lake, arid northwestern China. *J. Limnol.* **2019**, *78*, 201–209. [[CrossRef](#)]
16. Liu, W.; Ma, L.; Abuduwaili, J. Anthropogenic Influences on Environmental Changes of Lake Bosten, the Largest Inland Freshwater Lake in China. *Sustainability* **2020**, *12*, 711. [[CrossRef](#)]
17. Zhang, F.; Yao, S.; Xue, B.; Lu, X.; Gui, Z. Organic carbon burial in Chinese lakes over the past 150 years. *Quat. Int.* **2017**, *438*, 94–103. [[CrossRef](#)]
18. Tarasov, P.E.; Demske, D.; Leipe, C.; Long, T.; Müller, S.; Hoelzmann, P.; Wagner, M. An 8500-year palynological record of vegetation, climate change and human activity in the Bosten Lake region of Northwest China. *Palaeogeogr. Palaeoclimatol. Palaeoecol.* **2019**, *516*, 166–178. [[CrossRef](#)]
19. En, Z.K.; Xu, H.; Lan, J.H.; Yan, D.N.; Sheng, E.G.; Yu, K.K.; Fu, P.Q.; Xu, S. Variable Late Holocene 14C Reservoir Ages in Lake Bosten, Northwestern China. *Front. Earth Sci.* **2019**, *7*, 328.
20. Yu, Z.; Wang, X.; Zhao, C.; Lan, H. Carbon burial in Bosten Lake over the past century: Impacts of climate change and human activity. *Chem. Geol.* **2015**, *419*, 132–141. [[CrossRef](#)]
21. Chen, F.; Huang, X.; Zhang, J.; Holmes, J.A.; Chen, J. Humid Little Ice Age in arid central Asia documented by Bosten Lake, Xinjiang, China. *Sci. China Ser. D Earth Sci.* **2006**, *49*, 1280–1290. [[CrossRef](#)]
22. Mischke, S.; Wünnemann, B. The Holocene salinity history of Bosten Lake (Xinjiang, China) inferred from ostracod species assemblages and shell chemistry: Possible palaeoclimatic implications. *Quat. Int.* **2006**, *154–155*, 100–112. [[CrossRef](#)]
23. Lei, X.; Lu, J.; Liu, Z.; Tong, Y.; Li, S. Concentration and distribution of antibiotics in water–sediment system of Bosten Lake, Xinjiang. *Environ. Sci. Pollut. Res.* **2015**, *22*, 1670–1678. [[CrossRef](#)]
24. Chen, J.; Zhang, E.; Brooks, S.J.; Huang, X.; Wang, H.; Liu, J.; Chen, F. Relationships between chironomids and water depth in Bosten Lake, Xinjiang, northwest China. *J. Paleolimnol.* **2014**, *51*, 313–323. [[CrossRef](#)]
25. Zhou, L.; Zhou, Y.; Hu, Y.; Cai, J.; Bai, C.; Shao, K.; Gao, G.; Zhang, Y.; Jeppesen, E.; Tang, X. Hydraulic connectivity and evaporation control the water quality and sources of chromophoric dissolved organic matter in Lake Bosten in arid northwest China. *Chemosphere* **2017**, *188*, 608–617. [[CrossRef](#)]
26. Zhang, L.; Zhao, T.; Shen, T.; Gao, G. Seasonal and spatial variation in the sediment bacterial community and diversity of Lake Bosten, China. *J. Basic Microbiol.* **2019**, *59*, 224–233. [[CrossRef](#)]
27. Shen, B.; Wu, J.; Zhao, Z. Organochlorine pesticides and polycyclic aromatic hydrocarbons in water and sediment of the Bosten Lake, Northwest China. *J. Arid. Land* **2017**, *9*, 287–298. [[CrossRef](#)]
28. Tang, X.; Xie, G.; Shao, K.; Dai, J.; Chen, Y.; Xu, Q.; Gao, G. Bacterial community composition in oligosaline lake Bosten: Low overlap of betaproteobacteria and bacteroidetes with freshwater ecosystems. *Microbes Environ.* **2015**, *30*, 180–188. [[CrossRef](#)]
29. Tang, X.; Xie, G.; Shao, K.; Bayartu, S.; Chen, Y.; Gao, G. Influence of Salinity on the Bacterial Community Composition in Lake Bosten, a Large Oligosaline Lake in Arid Northwestern China. *Appl. Environ. Microbiol.* **2012**, *78*, 4748. [[CrossRef](#)]
30. Dai, J.; Tang, X.; Gao, G.; Chen, D.; Shao, K.; Cai, X.; Zhang, L. Effects of salinity and nutrients on sedimentary bacterial communities in oligosaline Lake Bosten, northwestern China. *Aquat. Microb. Ecol.* **2013**, *69*, 123–134. [[CrossRef](#)]
31. Song, W.; Qi, R.; Zhao, L.; Xue, N.; Wang, L.; Yang, Y. Bacterial community rather than metals shaping metal resistance genes in water, sediment and biofilm in lakes from arid northwestern China. *Environ. Pollut.* **2019**, *254*, 113041. [[CrossRef](#)] [[PubMed](#)]
32. Mamat, Z.; Haximu, S.; yong Zhang, Z.; Aji, R. An ecological risk assessment of heavy metal contamination in the surface sediments of Bosten Lake, northwest China. *Environ. Sci. Pollut. Res.* **2016**, *23*, 7255–7265. [[CrossRef](#)] [[PubMed](#)]
33. Liu, Y.; Mu, S.; Bao, A.; Zhang, D.; Pan, X. Effects of salinity and (an) ions on arsenic behavior in sediment of Bosten Lake, Northwest China. *Environ. Earth Sci.* **2015**, *73*, 4707–4716. [[CrossRef](#)]
34. Wufuer, R.; Liu, Y.; Mu, S.; Song, W.; Yang, X.; Zhang, D.; Pan, X. Interaction of dissolved organic matter with Hg(II) along salinity gradient in Boston Lake. *Geochem. Int.* **2014**, *52*, 1072–1077. [[CrossRef](#)]

35. Sun, P.; Zhang, Q.; Yao, R.; Singh, V.P.; Song, C. Low Flow Regimes of the Tarim River Basin, China: Probabilistic Behavior, Causes and Implications. *Water* **2018**, *10*, 470. [CrossRef]
36. Liu, Y.; Chen, Y. Saving the “Green Corridor”: Recharging groundwater to restore riparian forest along the lower Tarim River, China. *Ecol. Restor.* **2007**, *25*, 112–117. [CrossRef]
37. Sun, J.; Zhang, Z.; Zhang, L. New evidence on the age of the Taklimakan Desert. *Geology* **2009**, *37*, 159–162. [CrossRef]
38. Sun, J.; Liu, T. The age of the Taklimakan Desert. *Science* **2006**, *312*, 1621. [CrossRef]
39. Liu, Y.; Bao, A. Exploring the Effects of Hydraulic Connectivity Scenarios on the Spatial-Temporal Salinity Changes in Bosten Lake through a Model. *Water* **2020**, *12*, 40. [CrossRef]
40. Wu, J.; Liu, W.; Zeng, H.; Ma, L.; Bai, R. Water Quantity and Quality of Six Lakes in the Arid Xinjiang Region, NW China. *Environ. Process.* **2014**, *1*, 115–125. [CrossRef]
41. Liu, Y.; Bao, A.; Chen, X.; Zhong, R. A Model Study of the Discharges Effects of Kaidu River on the Salinity Structure of Bosten Lake. *Water* **2019**, *11*, 8. [CrossRef]
42. Chen, X.; Wu, J.; Hu, Q. Simulation of climate change impacts on streamflow in the Bosten Lake Basin using an artificial neural network model. *J. Hydrol. Eng.* **2008**, *13*, 180–183. [CrossRef]
43. Wu, J.; Ma, L.; Zeng, H. Water quality and quantity characteristics and its evolution in Lake Bosten, Xinjiang over the past 50 years. *Sci. Geogr. Sin.* **2013**, *33*, 231–237.
44. Tiwari, A.K.; Pisciotta, A.; De Maio, M. Evaluation of groundwater salinization and pollution level on Favignana Island, Italy. *Environ. Pollut.* **2019**, *249*, 969–981. [CrossRef] [PubMed]
45. Elzien, S.; Mohamed, S.; Keiralla, K.; Attaj, O.; Hussein, H. Hydro-geochemical Signature in the Thermal Waters in Jebel Mara, Darfur Region Western Sudan. *J. Geol. Geosci.* **2013**, *3*, 138.
46. Wilcox, L. *Classification and Use of Irrigation Waters*; USDA Circular No. 969; United States Department of Agriculture: Washington, DC, USA, 1955; p. 19.
47. Sharma, P.; Sarma, H.P.; Mahanta, C. Evaluation of groundwater quality with emphasis on fluoride concentration in Nalbari district, Assam, Northeast India. *Environ. Earth Sci.* **2012**, *65*, 2147–2159. [CrossRef]
48. Saleh, A.; Al-Ruwaih, F.; Shehata, M. Hydrogeochemical processes operating within the main aquifers of Kuwait. *J. Arid. Environ.* **1999**, *42*, 195–209. [CrossRef]
49. Wang, X.; Ozdemir, O.; Hampton, M.A.; Nguyen, A.V.; Do, D.D. The effect of zeolite treatment by acids on sodium adsorption ratio of coal seam gas water. *Water Res.* **2012**, *46*, 5247–5254. [CrossRef]
50. Zhang, B.; Song, X.; Zhang, Y.; Han, D.; Tang, C.; Yu, Y.; Ma, Y. Hydrochemical characteristics and water quality assessment of surface water and groundwater in Songnen plain, Northeast China. *Water Res.* **2012**, *46*, 2737–2748. [CrossRef]
51. Nazzal, Y.; Ahmed, I.; Al-Arifi, N.S.N.; Ghrefat, H.; Zaidi, F.K.; El-Waheidi, M.M.; Batayneh, A.; Zumlot, T. A pragmatic approach to study the groundwater quality suitability for domestic and agricultural usage, Saq aquifer, northwest of Saudi Arabia. *Environ. Monit. Assess.* **2014**, *186*, 4655–4667. [CrossRef]
52. Subramani, T.; Elango, L.; Damodarasamy, S.R. Groundwater quality and its suitability for drinking and agricultural use in Chithar River Basin, Tamil Nadu, India. *Environ. Geol.* **2005**, *47*, 1099–1110. [CrossRef]
53. Hossain, M.; Patra, P.K. Water pollution index—A new integrated approach to rank water quality. *Ecol. Indic.* **2020**, *117*, 106668. [CrossRef]
54. WHO. *Guidelines for Drinking-Water Quality*, 4th ed. 2011. Available online: http://whqlibdoc.who.int/publications/2011/9789241548151_eng.pdf (accessed on 6 January 2019).
55. Ministry of Health of the People’s Republic of China; Standardization Administration of the People’s Republic of China. *China National Standards for Drinking Water Quality*; GB5749-2006; Ministry of Health of the People’s Republic of China, Standardization Administration of the People’s Republic of China: Beijing, China, 2006.
56. Ye, C.; Butler, O.M.; Du, M.; Liu, W.; Zhang, Q. Spatio-temporal dynamics, drivers and potential sources of heavy metal pollution in riparian soils along a 600 kilometre stream gradient in Central China. *Sci. Total Environ.* **2019**, *651*, 1935–1945. [CrossRef] [PubMed]
57. ter Braak, C.J.F.; Smilauer, P. *Canoco Reference Manual and User’s Guide: Software for Ordination, Version 5.0*; Microcomputer Power: Ithaca, NY, USA, 2012; pp. 1–496.
58. Mueller, T.; Pusuluri, N.; Mathias, K.; Cornelius, P.; Barnhisel, R.; Shearer, S. Map quality for ordinary kriging and inverse distance weighted interpolation. *Soil Sci. Soc. Am. J.* **2004**, *68*, 2042–2047. [CrossRef]

59. Li, Z.; Yang, Q.; Yang, Y.; Xie, C.; Ma, H. Hydrogeochemical controls on arsenic contamination potential and health threat in an intensive agricultural area, northern China. *Environ. Pollut.* **2020**, *256*, 113455. [[CrossRef](#)]
60. Boyd, C.E.; Tucker, C.S. Water quality. In *Aquaculture: Farming Aquatic Animals and Plants*; John Wiley & Sons: Chichester, West Sussex, UK, 2019; pp. 63–92.
61. Gibbs, R.J. Mechanisms controlling world water chemistry. *Science* **1970**, *170*, 1088–1090. [[CrossRef](#)]
62. Zang, C.; Dame, J.; Nüsser, M. Hydrochemical and environmental isotope analysis of groundwater and surface water in a dry mountain region in Northern Chile. *Environ. Monit. Assess.* **2018**, *190*, 334. [[CrossRef](#)]
63. Nguyen, T.T.; Kawamura, A.; Tong, T.N.; Nakagawa, N.; Amaguchi, H.; Gilbuena, R. Clustering spatio-seasonal hydrogeochemical data using self-organizing maps for groundwater quality assessment in the Red River Delta, Vietnam. *J. Hydrol.* **2015**, *522*, 661–673. [[CrossRef](#)]
64. Parkhurst, D.L.; Appelo, C. *Description of Input and Examples for PHREEQC Version 3: A Computer Program for Speciation, Batch-Reaction, One-Dimensional Transport, and Inverse Geochemical Calculations*; US Geological Survey: Reston, VA, USA, 2013; pp. 2328–7055.
65. Li, Y. Characteristics of Kaidu River Water Quality Changes along the Course (in Chinese). *Henan Water Conserv. South-to-North Water Divers.* **2010**, *7*, 69–71.
66. Ma, L.; Abuduwaili, J.; Li, Y.; Abdyzhaparuulu, S.; Mu, S. Hydrochemical Characteristics and Water Quality Assessment for the Upper Reaches of Syr Darya River in Aral Sea Basin, Central Asia. *Water* **2019**, *11*, 1893. [[CrossRef](#)]
67. Cheng, L.; Xue, B.; Zawisza, E.; Yao, S.; Liu, J.; Li, L. Effects of environmental change on subfossil Cladocera in the subtropical shallow freshwater East Taihu Lake, China. *Catena* **2020**, *188*, 104446. [[CrossRef](#)]
68. Lazzari, N.; Martín-López, B.; Sanabria-Fernandez, J.A.; Becerro, M.A. Alpha and beta diversity across coastal marine social-ecological systems: Implications for conservation. *Ecol. Indic.* **2020**, *109*, 105786. [[CrossRef](#)]
69. Pollice, A.; Jona-Lasinio, G.; Gaglio, M.; Blanchet, F.G.; Fano, E.A. Modelling the effect of directional spatial ecological processes for a river network in Northern Italy. *Ecol. Indic.* **2020**, *112*, 106144. [[CrossRef](#)]
70. Li, H.; Cai, Y.; Gu, Z.; Yang, Y.-L.; Zhang, S.; Yang, X.-L.; Song, H.-L. Accumulation of sulfonamide resistance genes and bacterial community function prediction in microbial fuel cell-constructed wetland treating pharmaceutical wastewater. *Chemosphere* **2020**, *248*, 126014. [[CrossRef](#)]
71. Shao, T.; Wang, T. Effects of land use on the characteristics and composition of fluvial chromophoric dissolved organic matter (CDOM) in the Yiluo River watershed, China. *Ecol. Indic.* **2020**, *114*, 106332. [[CrossRef](#)]
72. Liu, Y.; Cheng, D.; Xue, J.; Weaver, L.; Wakelin, S.A.; Feng, Y.; Li, Z. Changes in microbial community structure during pig manure composting and its relationship to the fate of antibiotics and antibiotic resistance genes. *J. Hazard. Mater.* **2020**, *389*, 122082. [[CrossRef](#)]
73. Kamal, M.; Ghaly, A.; Mahmoud, N.; Cote, R. Phytoaccumulation of heavy metals by aquatic plants. *Environ. Int.* **2004**, *29*, 1029–1039. [[CrossRef](#)]
74. Wang, W.-X.; Rainbow, P.S. Comparative approaches to understand metal bioaccumulation in aquatic animals. *Comp. Biochem. Physiol. C: Toxicol. Pharmacol.* **2008**, *148*, 315–332. [[CrossRef](#)]
75. Rzymiski, P.; Klimaszuk, P.; Niedzielski, P.; Marszelewski, W.; Borowiak, D.; Nowiński, K.; Baikenzheyeva, A.; Kurmanbayev, R.; Aladin, N. Pollution with trace elements and rare-earth metals in the lower course of Syr Darya River and Small Aral Sea, Kazakhstan. *Chemosphere* **2019**, *234*, 81–88. [[CrossRef](#)]
76. Podgorski, J.; Berg, M. Global threat of arsenic in groundwater. *Science* **2020**, *368*, 845–850. [[CrossRef](#)]

Publisher’s Note: MDPI stays neutral with regard to jurisdictional claims in published maps and institutional affiliations.



© 2020 by the authors. Licensee MDPI, Basel, Switzerland. This article is an open access article distributed under the terms and conditions of the Creative Commons Attribution (CC BY) license (<http://creativecommons.org/licenses/by/4.0/>).